Assessment of Predictive Capability of Aeromechanics Methods

William G. Bousman*
Quercus Associates SL
Menlo Park, CA

Thomas Norman
NASA Ames Research Center
Moffett Field, CA

A technique is described based on simple statistics that can be used to assess the accuracy of analytical predictions compared to measurements. It is demonstrated that the approach can be applied to a broad range of problems in the area of helicopter aeromechanics, including hover and forward flight performance, blade aerodynamic and structural loads, vibratory forces, and aeroelastic/aeromechanical stability. The method described has both strengths and weaknesses, and these are shown with examples and discussed. It is also shown that there is currently a hierarchy of accuracy in aeromechanics problems, ranging from the necessarily accurate methods for performance prediction to the inaccurate and untrustworthy calculations of fixed-system vibration.

Nomenclature

A	rotor disk area, ft^2
C_{CM}	chord bending moment coefficient, $M_C/\rho AV_T^2\,R$
C_{FM}	flap bending moment coefficient, $M_F/\rho AV_T^2\,R$
C_P	power coefficient, $P/\rho AV_T^3$ or pressure coefficient
C_T	thrust coefficient, $T/\rho AV_T^2$
C_{TM}	torsion bending moment coefficient, $M_T/\rho AV_T^2\,R$
C_W	weight coefficient, $GW/\rho AV_T^2$
c_m	section pitching moment coefficient
c_n	section normal force coefficient
GW	gross weight, lb
M	section Mach number
M_C	chord bending moment, inch-lb
M_F	flap bending moment, inch-lb
M_T	torsion moment, inch-lb
m	slope, linear regression
P	power, hp
P_H	power to hover, hp
R	blade radius, inches
r	section radius, inches
S_e	standard error of estimate, linear regression
T	rotor thrust, lb
V_H	ideal induced velocity in hover, ft/s
V_{ROC}	vertical rate of climb, ft/s
V_T	rotor tip speed, ft/s
μ	advance ratio
ρ	density of air, slugs/ft^3
σ	standard deviation or rotor solidity

Introduction

Under NASA's Subsonic Rotary Wing (SRW) Project, a detailed assessment of the predictive accuracy of numerous analytical methods has been made, including those methods dealing with aeromechanics, acoustics, experimental methods, flight dynamics and control, propulsion, and structures and materials. Within the general area of aeromechanics, this assessment has been divided into two parts, the first dealing with classical methods embodied in comprehensive analyses and the second dealing with computational fluid dynamics (CFD) with a particular emphasis on coupled computational fluid dynamics/computational structural dynamics methods, and Navier–Stokes representations of the aerodynamic forces. The present paper addresses the first part of the aeromechanics assessment, that dealing with classical methods.

Progress in the aeromechanics disciplines over the past 70 to 80 years has been substantial, yet there have been few attempts at a quantitative assessment of analytical methods (Refs. 1–3). Some 30 or more years ago, at the Dynamic Specialists Meeting at Ames Research Center, Dick Bennett said ". . . correlation, like beauty, is in the eye of the beholder" (Ref. 4). These words, a fine example of Dr. Bennett's wit, have lingered in the engineering community for decades. Yet his statement has been taken out of context. Dick used these words as an example of fuzzy thinking and in the next sentence he stated, "So we must come up with a good definition, a workable definition of correlation."

The primary purpose of this paper is to present one approach to quantitative correlation, using the work that has been done under NASA's SRW project. Beyond that primary purpose, it will also be shown that the use of quantitative correlation provides insight into the accuracy of present analytical methods when applied over a range of aeromechanics problems.

Methodology for Quantitative Correlation

A standardized approach to the quantitative assessment of predictive accuracy of analytical methods is described here. The basic approach is

*Corresponding author; email: barlowi@earthlink.net.
Presented at the AHS Specialist's Conference on Aeromechanics, San Francisco, CA, January 23–25, 2008. Received May 2008; accepted June 2009.

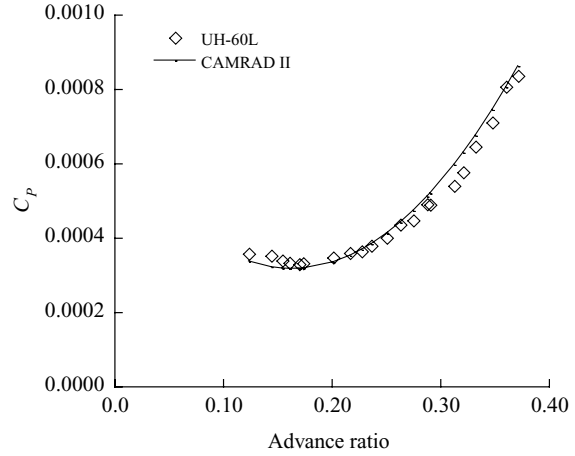

Fig. 1. UH-60L with standard blades. Power coefficient as a function of advance ratio; $C_W/\sigma = 0.0787$ (Ref. 5).

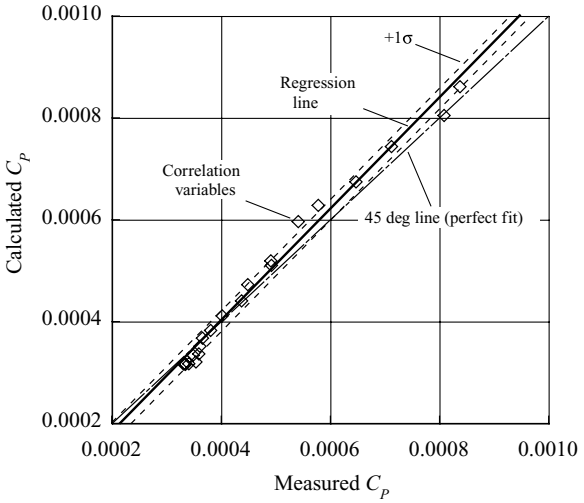

Fig. 2. Predictive accuracy of CAMRAD II for UH-60L with standard blades for $C_W/\sigma = 0.0787$; $m = 1.093$, $S_e = \pm 1\%$ (Ref. 5).

to plot the calculation of an appropriate parameter as a function of its measurement. Exact correlation is obtained if all the calculated and measured points lie on a 45° line. This approach is illustrated in Figs. 1 and 2. Figure 1 shows the measured and calculated aircraft power coefficients, C_P, for advance ratios from about 0.15–0.35 for a UH-60L with standard blades. The aircraft weight coefficient in this case, C_W/σ, is about 0.079. The calculations have been made using CAMRAD II (Ref. 5). A qualitative examination of Fig. 1 shows that there is fairly good agreement between analysis and data, but the power is underpredicted at low speeds and overpredicted for $0.25 \leq \mu \leq 0.35$. Figure 2 shows the calculated C_P as a function of the measured C_P for the data. A linear regression line is calculated for the correlation points and is shown as a solid line bracketed by dashed lines that represent the scatter of the data. The scatter is indicated by $\pm S_e$ (the standard error of estimate, which is equivalent to $\pm 1\sigma$). The scatter in this case is a little more than 1% (based on the ordinate scale), which is typical of better performance calculations. At low power coefficients, there is an underprediction in Fig. 2, whereas at high power coefficients there is an overprediction, as was noted for Fig. 1. The slope of the linear regression line is 1.093 in this case. In this assessment approach, slopes greater than 1.0 are considered an overprediction and slopes less than 1.0 are an underprediction.

The scatter in the correlation in the example in Fig. 2 is presumably caused by measurement errors. But the difference in the slope of the regression line, in this case an overprediction, may be caused by errors in analysis or measurement.

In this example, the power coefficient varies over a range of about $2.5x$, which provides a reasonable assessment of the correlation. If this range or ratio were close to $1.0x$, the lack of variation would be so limited that the regression fit would be meaningless. In the example shown in Fig. 1, the variation in the power coefficient is caused by changes in airspeed, but it is generally not important what the source of the variation is.

In the example of Fig. 2, the scatter is quite low, and quantitatively the predictive accuracy is usefully judged by the slope, $m = 1.093$. But in other cases, as will be shown later, the scatter may be much larger and this scatter may be more significant in assessing the accuracy of the prediction. Moreover, in other cases there will be a noticeable offset in values and this offset may be more important than either the slope or scatter.

It is useful in many cases to include additional independent variables and group comparisons together. Thus, for the UH-60L flight test data, power coefficient data at other weight coefficients (airspeed sweeps) can be used, and the data are combined or grouped together, which may provide a better test, as suggested by Fig. 3. In this example, data and calculations from four airspeed sweeps are combined and the overall slope is 1.024, indicating a calculation accuracy of +2.4%.

The combined analysis of the four airspeed sweeps in Fig. 3 is perhaps a better estimate of the predictive accuracy of CAMRAD II, since a wider parameter variation is used in the assessment. But in some cases, combining data sets can obscure trends that may be important. Table 1 shows the slopes and scatter for the four airspeed sweeps used in Fig. 3.

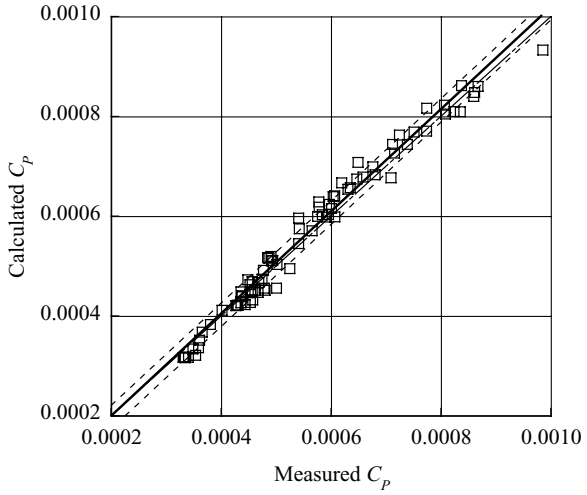

Fig. 3. Predictive accuracy of CAMRAD II for UH-60L with standard blade for four weight coefficients (Ref. 5); $m = 1.024$, $S_e = \pm 2\%$.

Table 1. Predictive accuracy of CAMRAD II for UH-60L with standard blade for four weight coefficients (Ref. 5)

C_W/σ	m	$\pm S_e$ (%)
0.0787	1.093	1.4
0.0981	1.003	1.6
0.1029	1.034	1.4
0.1211	0.848	1.7

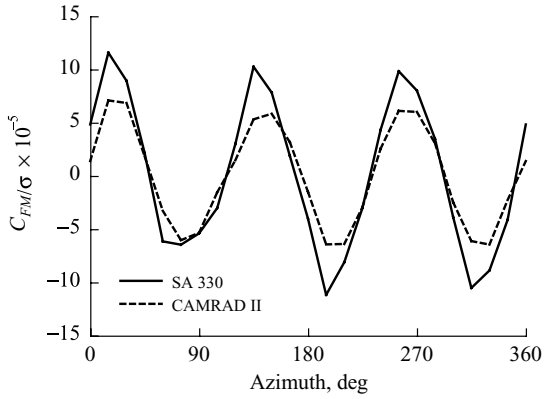

Fig. 4. SA 330 (Puma) nondimensional vibratory flap bending moment as a function of blade azimuth at $0.46R$ and $\mu = 0.362$ (Ref. 6).

For the three lower C_W/σ values, the overprediction varies from 0.3% to 9.3%. But for the highest weight coefficient, there is a 15.2% underprediction. The scatter is relatively unchanged, but the change in slope suggests that the calculation has degraded at high blade loading, perhaps because of dynamic stall.

The choice of a relevant parameter for quantitative correlation can be difficult. For performance, the choice of the power required at a single test point is straightforward. But for that same test point, it is not so clear how to represent the blade aerodynamic or structural loads. Figure 4 compares the measured and predicted nondimensional vibratory flap bending moment for the research Puma (Ref. 6). What number or numbers are the best choice to represent this correlation? The peak-to-peak loads describe the total amplitude of the flap bending moment but do not describe the frequency content, either in amplitude (generally) or phase. The approach used here is to examine the predictive accuracy by sampling the data every 15 deg, which represents the frequency content of the measured time history. Thus, the blade azimuth is treated as the independent variable. The resulting linear regression for this example is shown in Fig. 5. The vibratory loads in this case are underpredicted by about 35%, which is also clearly seen in the time history in Fig. 4. The scatter is about ±7%, which is an increase from that observed in the UH-60L performance results in Fig. 3, but as will be shown below is quite good for structural load prediction.

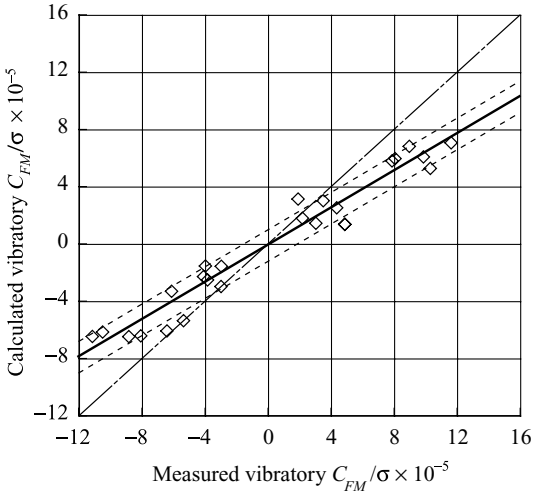

Fig. 5. SA 330 (Puma) linear regression of nondimensional vibratory flap bending moment at $0.46R$ and $\mu = 0.362$ (Ref. 6); $m = 0.649$, $S_e = \pm 7\%$.

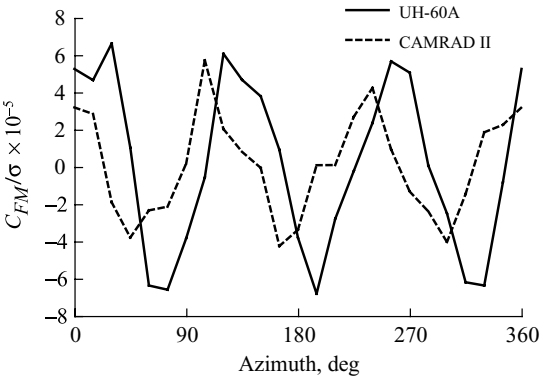

Fig. 6. UH-60A nondimensional vibratory flap bending moment as a function of blade azimuth at $0.50R$ and $\mu = 0.368$ (Ref. 6).

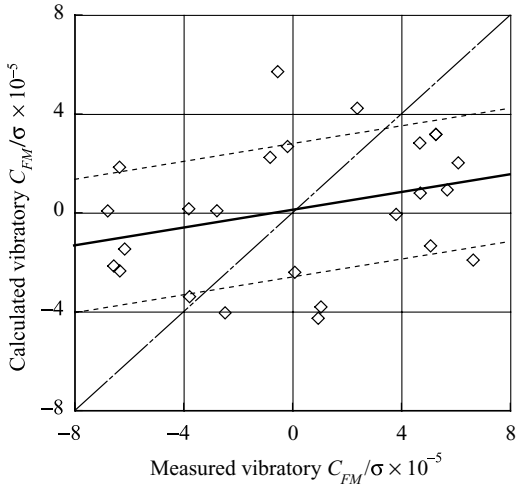

Fig. 7. UH-60A linear regression of nondimensional vibratory flap bending moment at $0.50R$ and $\mu = 0.368$ (Ref. 6); $m = 0.180$, $S_e = \pm 17\%$.

But what happens when there is a phase shift in the structural loads? Figure 6 shows a correlation case for the vibratory flap bending moment for the UH-60A that includes a substantial phase shift. The predicted amplitude in this case appears to be about 75% of the measurement, but the phase difference has a severe effect on the linear regression fit as shown in Fig. 7. Because of the phase difference the scatter is increased and the slope of the linear regression fit is essentially meaningless. The examples shown in Figs. 6 and 7 provide a warning that the present methodology is sensitive to some aspects of correlation, particularly phase differences (which may be a good thing).

Aeromechanics Topics

The remainder of this paper will look at a wide range of aeromechanics topics using the quantitative correlation approach described here. Topics range from basic rotorcraft performance, in both hover and forward flight, aerodynamic loads on the blade and fuselage, structural loads, vibration, and rotor stability along with a few miscellaneous topics. In selecting these topics, only results from the published literature have been used. An effort has been made to use data sets where one analysis has been

used for many different experimental cases, and the investigators have applied their method in a uniform manner.

Although a broad range of topics are included here, the predictions of only a limited number of comprehensive analyses have been examined. There are many other codes that are available, and the examination of their predictive capability would be valuable. Moreover, the examination of additional cases would provide a better evaluation of the applicability of the present method.

In some cases words may be used here such as error, discrepancy, or difference, and these words are used interchangeably. But it is important to recognize that differences between measurement and calculation may be caused by errors in the calculation, errors in the measurements, or errors in both. When reasonably good correlation is obtained, as is the case currently for flight performance, it will be pointed out that improvement in calculation accuracy cannot be obtained until significant improvements are made in measurement accuracy. But in other cases, the need for improvement lies with analysis.

Hover performance

Felker et al. (Ref. 7) applied the hover performance code EHPIC to a broad range of rotor tests, including four main rotors, two tail rotors, and three tiltrotors. The EHPIC code is a lifting surface analysis that uses a free wake. Drag is determined using table lookup. More or less typical of the basic hover performance data used in Ref. 7, Fig. 8 shows the measured power coefficient as a function of thrust coefficient for the Boeing prototype YUH-61A main rotor tested on a whirl tower along with the EHPIC code prediction (consult Ref. 7 for the original data sources). The range of power coefficient values in this case is about $4.9x$.

The accuracy of the EHPIC code for four main rotors is shown in Fig. 9. For the combined analysis, the underprediction is about 1.5% and the scatter is low. The four rotors analyzed include a two-bladed rotor with significant taper that was tested about 1958 and is referred to as the TN 4357 rotor (TN 4357 was the NACA technical note wherein the data were published). This rotor, 53.6-ft in diameter, was tested on a whirl tower with a height-to-diameter ratio of 0.78. Because of ground plane effects, the data were corrected (about 5%). Two different tip Mach numbers are included in the data set. The second data set was for a three-bladed rotor, tested about 1951, and is referred to as the TN 2277 rotor. This rotor was untapered and had a 38-ft diameter. As with the two-bladed test, two different tip Mach numbers were tested. The third data set was for a CH-47B rotor tested on a whirl tower, also with three blades. The fourth data set was for the four-bladed YUH-61A rotor, also tested on a whirl tower (see Fig. 8). Table 2 compares the accuracy metrics for the four data sets. The hover performance is underpredicted for all main rotors, ranging from 7.2% to 2.7%.

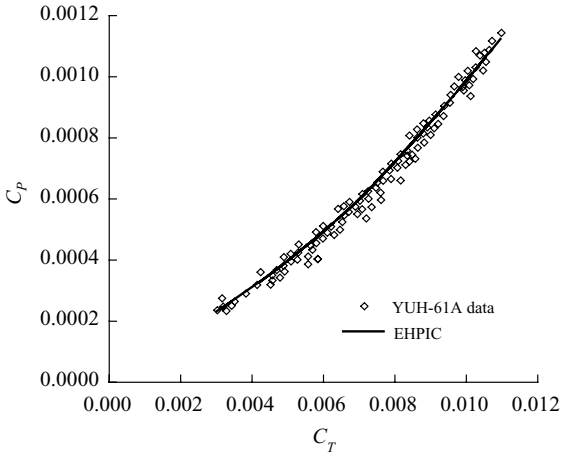

Fig. 8. C_P as a function of C_T for the Boeing YUH-61A main rotor tested on a whirl tower compared to EHPIC code (Ref. 7).

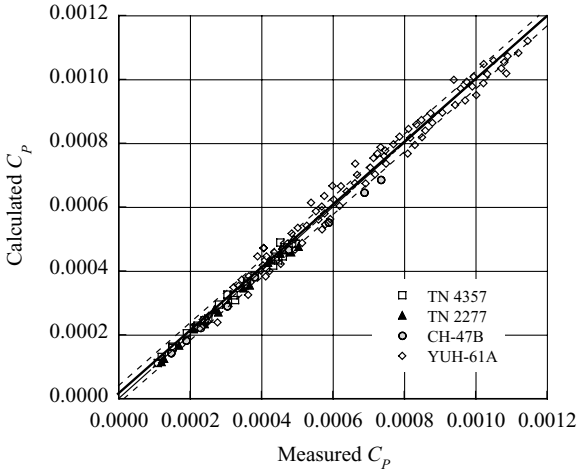

Fig. 9. Accuracy of EHPIC hover prediction for four main rotors (Ref. 7); $m = 0.985$, $S_e = \pm 2\%$.

Table 2. Accuracy of EHPIC for hover performance of four main rotors (Ref. 7)

Main Rotor	Blade No.	m	$\pm S_e$ (%)
TN 4357	2	0.973	1.0
TN 2277	3	0.971	0.9
CH-47B	3	0.927	1.3
YUH-61A	4	0.966	2.6

Kocurek et al. (Ref. 2) evaluated the Bell Helicopter Textron hover prediction methodology in the late 1970s. Their analysis used a lifting surface method with an empirical wake model. They evaluated a number of isolated rotor data sets, but also included flight test results from 13 helicopters. Thus, their analysis calculated not only hover performance but also fuselage download, tail rotor power, accessory losses, and transmission losses. They found that the differences between measured and predicted power varied for the most part between -3.2 and $+3.2\%$. It appears that predictive accuracy has not substantially changed in the past 30 years or so. At the beginning of this paper, it was stated that the quantitative evaluation of predictive accuracy may benefit from comparisons with multiple data sets. But as analytical methods become more accurate, the use of multiple data sets may be counterproductive because of unknown errors in some of these data sets.

Vertical rate of climb

The U.S. Army requires a minimum maneuver capability at its design hover ceiling, usually expressed as a 500-ft/min vertical rate of climb (VROC). Harris (Ref. 8) has pointed out that the accuracy of power prediction for a vertical climb is poor. He included flight test data in Ref. 8 from the OH-58D development program, and these data have been used by Felker et al. (Ref. 7) to examine the accuracy of the EHPIC code for VROC prediction. Figure 10 shows the power ratio in a vertical climb as a function of the nondimensional climb rate. At these low climb rates (a $V_{\mathrm{ROC}}/V_H \sim 0.3$ is equivalent to a 500-ft/min climb), the EHPIC

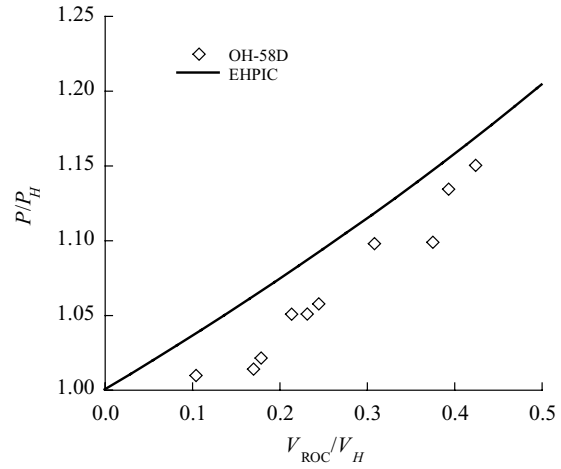

Fig. 10. OH-58D vertical rate-of-climb, power ratio as a function of nondimensional climb rate (Ref. 7).

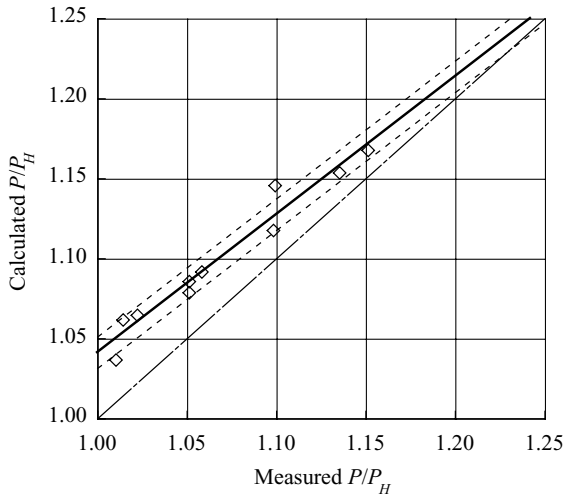

Fig. 11. Accuracy of EHPIC vertical rate-of-climb prediction for OH-58D (Ref. 7); $m = 0.862$, $S_e = \pm 1\%$.

code overpredicts the power required. This is shown more clearly in Fig. 11, which shows the linear regression fit to the data. The slope of the regression line indicates a 14% underprediction, but the accuracy in this case is dominated by the offset rather than the slope. Thus, the average offset, which is about +2.5% high, is the best measure of the correlation inaccuracy for this case. In most cases treated in this paper, however, it did not appear that the offset was important.

Forward flight performance

The calculation of forward flight performance is particularly important at the maximum flight speed or at the best cruise speed, either of which may be a contractual guarantee. Yeo et al. (Ref. 5) have used CAMRAD II to look at three sets of flight test data on the UH-60: data obtained with the standard blades during the Airloads Program on the UH-60A (Ref. 9), data obtained with the standard blades during a subsequent development program using the UH-60L, and data obtained on a UH-60L with wide chord blades (see Ref. 5 for discussion of data sources). Figure 12 shows power coefficient calculations and measurements for the UH-60A (the data for the airspeed at $C_W/\sigma = 0.090$ are

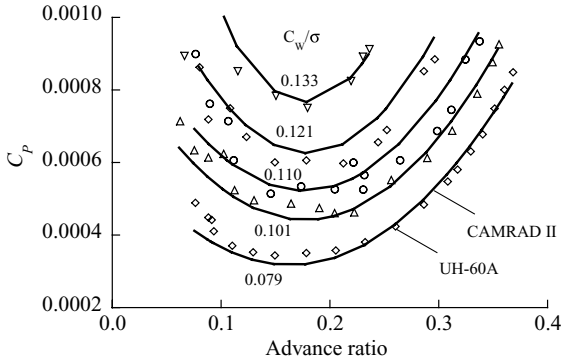

Fig. 12. UH-60A C_P as a function of μ for five weight coefficients (airspeed sweeps) compared with CAMRAD II (Ref. 5).

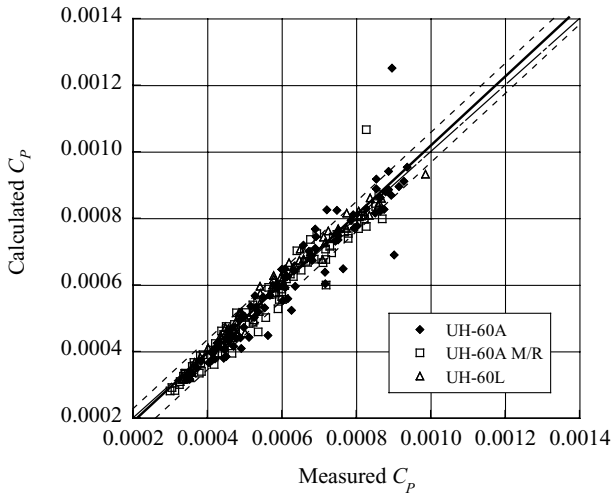

Fig. 13. Accuracy of CAMRAD II for the three standard blade data sets (Ref. 5); $m = 1.037$, $S_e = \pm 3\%$.

not included for clarity), and these show the typical form of the power required curve with airspeed and increasing weight. The accuracy of this calculation as well as calculations from the UH-60L tests with the standard blade is shown in Fig. 13. For the UH-60A data, there are two independent measurements of power. First, there is the power that is measured at the engine output shafts, which represents the total vehicle power and, second, there is the power based on the main rotor torque measurement. These two sets of measurements are treated as independent data sets, and appropriate CAMRAD II calculations are made for the separate measurements. Hence Fig. 13 is a combined analysis of three data sets for the power required for a UH-60 with standard blades. There is an overprediction of power of 3.7%, and the scatter is high for performance measurements. In particular, some solution points are well away from the 45° line, generally those points at either end of the high weight coefficient speed sweeps.

Table 3 shows the individual accuracies for the three sets of data and also includes the accuracy values for the UH-60L with the wide chord blades (these data are proprietary and are not shown in Fig. 13). The total power for the UH-60A tested during the Airloads Program is overpredicted by 7.6%, and the scatter is excessive. Power based on the main rotor shaft torque is more accurate and is similar to the total power measurements on the UH-60L. The wide chord blade data are underpredicted by 13.2%, which is an excessive error for performance data for any

Table 3. Accuracy of CAMRAD II for three standard blade data sets plus wide chord blades (Ref. 5)

Aircraft	Rotor	m	$\pm S_e$ (%)
UH-60A	std	1.076	4.4
UH-60A (M/R power)	std	1.022	2.9
UH-60L	std	1.024	1.7
UH-60L	Wide chord	0.868	2.1

aircraft. The problems with the accuracy measurements shown later in Table 6 are caused in part by serious temperature calibration errors in the original flight test measurements that have not been resolved (Ref. 10). It may be the case that these flight test measurements are not suitable for the assessment of flight performance accuracy.

A generation ago, Harris et al. (Ref. 1) examined cruise performance predictions for 11 helicopters at various weight coefficients, providing 35 test cases. Of the 35, 18 were within a ±3% error band and 30 were within ±6%. No significant improvement in performance prediction has been demonstrated since 1979. If accuracies for forward flight performance are required that are better than Harris et al. demonstrated 35 years ago, then improved measurements will be needed.

Forward flight airloads

Few data sets include rotor blade airloads. Such experiments require chordwise arrays of pressure transducers, ideally at multiple radial stations. Older experiments, using differential pressure transducers, are able to compute normal force and pitching moment; whereas more recent experiments, employing arrays of absolute pressure transducers, also obtain chord force (but not viscous drag).

Yeo and Johnson (Ref. 11) have looked at five sets of rotor airloads data. Two of these data sets, that of the H-34 and the UH-60A, have measurements at radial stations along the blade span; whereas the other three data sets, flight tests of the research Puma, the SA 349/2, and model tests of the BO 105, have measurements at only a few stations near the blade tip. The correlation effort by Yeo and Johnson selected an outboard radial station from the five data sets, generally near $0.90R$, and then picked two airspeeds: a low speed was selected near $\mu \sim 0.15$, where there is strong loading from the vortex wake, and a high speed was selected that was representative of the maximum flight speed. For the H-34, flight-test data were used for the low-speed case, whereas wind tunnel data (same rotor) were used for the high-speed case. There was no high-speed case for the BO 105 wind tunnel tests.

The CAMRAD II calculations were made using two wake models: a rolled-up wake model and a multitrailer model. Otherwise, analysis options were held constant for all of the cases. Thus, there were nine test conditions (five rotors at low speed, four rotors at high speed) and two wake models, which resulted in 18 calculations for both normal force, M^2c_n, and pitching moment, M^2c_m. An example of the calculation for normal force for the research Puma at low speed is shown in Fig. 14. The time history is sampled every 15 deg so as to represent the frequency content. The combined analysis of the 18 cases is shown in Fig. 15. There is a general underprediction of about 17%, and the scatter is much greater than was seen for the performance calculations. If the low- and high-speed cases are examined separately, the combined results are much the same: at low speed, $m = 0.814$ and at high speed, $m = 0.839$. But if the accuracy of the individual rotors or helicopters is examined separately, the results are variable. They range from $m = 0.138$ for the low-speed BO 105 case to $m = 1.403$ for the low-speed Puma case. This range of variability makes it difficult to know whether the overall slope in Fig. 15 is representative of analysis accuracy.

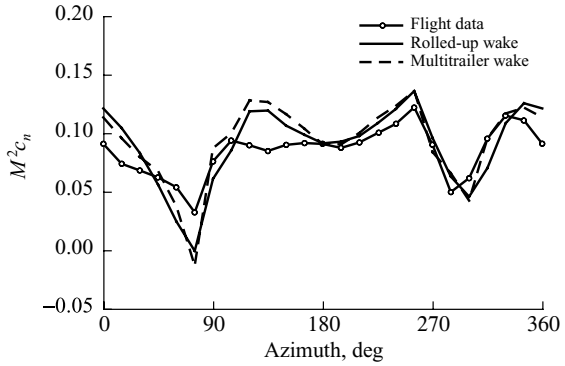

Fig. 14. Measured normal force as a function of azimuth on the research Puma compared with CAMRAD II (Ref. 11); $r/R = 0.92$, $\mu = 0.141$.

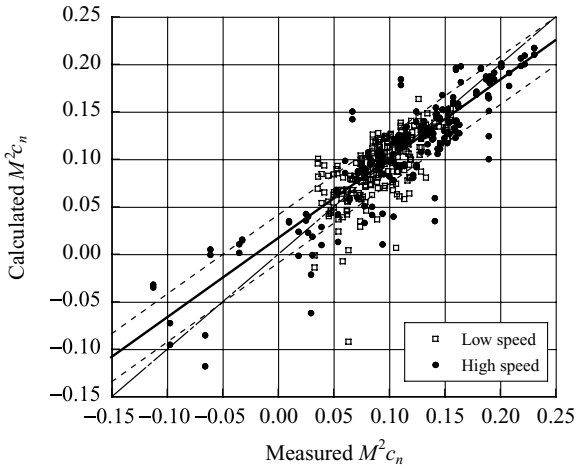

Fig. 15. Accuracy of CAMRAD II for combined analysis of five rotors at two airspeeds (Ref. 11); $m = 0.834$, $S_e = \pm 10\%$.

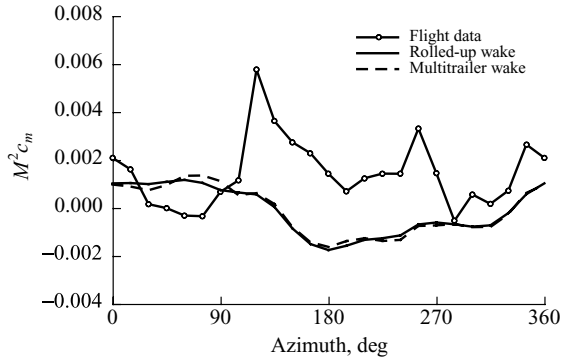

Fig. 16. Measured pitching moment as a function of azimuth on the SA 349/2 compared with CAMRAD II (Ref. 12); $r/R = 0.88$, $\mu = 0.14$.

Similar results are obtained by assessing the accuracy of the blade pitching moments. Figure 16 shows an example for the SA 349/2 where $\mu = 0.14$ and $r/R = 0.88$. This is 1 of 16 cases (there are no BO 105 data for pitching moment). The poor correlation indicates that the lifting-line model in CAMRAD II does not adequately represent the disk vortex loading for this low-speed case. The combined analysis of the 16 cases

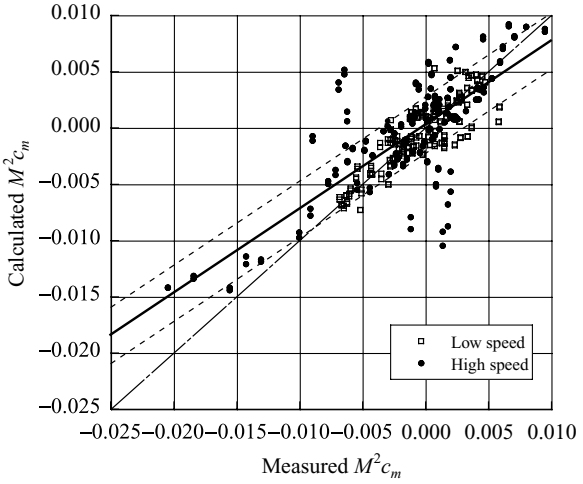

Fig. 17. Accuracy of CAMRAD II for combined analysis of four rotors at two airspeeds (Ref. 11); $m = 0.747$, $S_e = \pm 25\%$.

for pitching moment is shown in Fig. 17. The underprediction for pitching moment is about 25%, and the scatter is increased over that seen for normal force. In the normal force case, little difference was seen in the computed slope for the separate analyses of the low- and high-speed cases. But for pitching moment at low speed, $m = 0.828$ and $S_e = \pm 16\%$, whereas at high speed, $m = 0.727$ and $S_e = \pm 31\%$. Analysis of the accuracy of the individual rotors shows considerable variation, as was seen for normal force. The slopes vary from -0.040 for the SA 349/2 at low speed (see Fig. 16) to 1.029 for the H-34 at high speed.

Blade structural loads in forward flight

The correct calculation of blade structural loads, that is, the flap bending, chord bending, and torsion moments, is important for fatigue and vibration. Yeo and Johnson (Ref. 5) have used CAMRAD II to compare with the structural loads from the same five experiments that were examined for their airloads in the preceding section. For this effort, they selected loads measured roughly at the midspan on the blade. Again, the same two airspeeds were selected, one near $\mu \sim 0.15$, where there is strong loading from the vortex wake, and one at high speed. For the low-speed case, flight test data were used for the H-34, whereas for the high-speed case, wind tunnel data were used (same rotor, different tests). There was no high-speed case for the BO 105 wind tunnel tests.

The CAMRAD II calculations were made using two wake models: a rolled-up wake model and a multitrailer model. Otherwise, analysis options were held constant for all of the cases. Thus, there were 9 test conditions (5 rotors at low speed, 4 rotors at high speed) and two wake models, which resulted in 18 calculations each for the flap bending, chord bending, and torsion moments.

An example of flap bending moment on the research Puma at high speed is shown in Fig. 18. For the comparisons of structural loads, the mean values of the measurements and calculations have been removed. As with the blade airloads, the variation in the regression analysis is provided by sampling the time histories every 15 deg. The combined analysis of the 18 sets of comparison are shown in Fig. 19. Based on this combined analysis, there is an underprediction of 27%. The predictive accuracy in this case is less than was observed in the previous normal force comparisons. This is not surprising since the blade normal forces largely determine the flap bending moments. As with the previous normal force assessment, there is little difference between the low- and

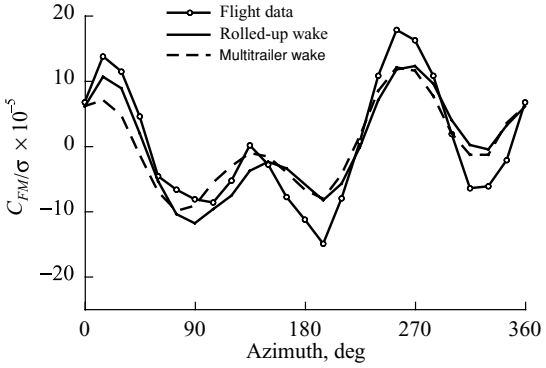

Fig. 18. Nondimensional flap bending moment as a function of azimuth on the Puma compared with CAMRAD II (Ref. 5); $r/R = 0.46$, $\mu = 0.362$.

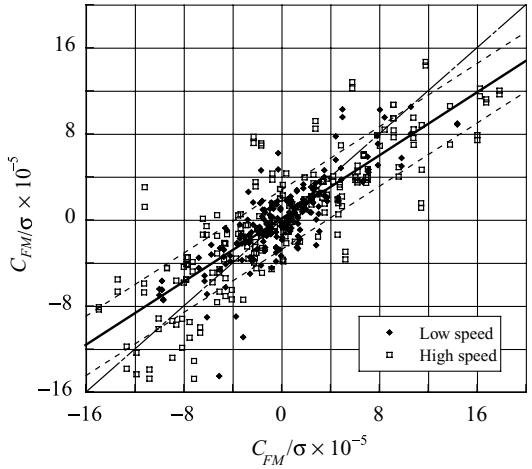

Fig. 19. Accuracy of CAMRAD II for combined analysis of midspan flap bending moment for five rotors at two airspeeds (Ref. 5); $m = 0.733$, $S_e = \pm 14\%$.

high-speed cases for flap bending moment, $m = 0.761$ at low speed and $m = 0.722$ high speed. Also, as seen for the airloads comparisons, there is a wide variation in the slope values for the 18 cases, the range at low speed extends from a slope of 0.372 for the BO 105 to 1.080 for the UH-60A.

An example of the CAMRAD II prediction of chord bending moment is shown in Fig. 20 for the SA 349/2 at high speed. The combined analysis of the 18 cases for chord bending is shown in Fig. 21. The combined accuracy in this case is poor. The underprediction of 73% is so large as to make the calculations largely untrustworthy. There are differences between the airspeed regimes, with a 64% underprediction at low speed and 75% at high speed. The variation between individual cases ranges from -86% for the Puma to -25% for the SA 349/2 (both at high speed).

It is expected that the chord bending calculation will be influenced by the rotor's lead–lag damper, particularly at inboard locations. The H-34, research Puma, and UH-60A all use hydraulic dampers that have strong nonlinearities. The SA 349/2 uses an elastomeric damper with weaker nonlinearities. The BO 105 does not have a damper, but there is probably some friction damping in the blade root attachment. But the differences in predictive accuracy for chord bending for these five rotors bear no obvious relationship to the damper type.

An example of CAMRAD II calculation of torsion moment for the UH-60A is shown in Fig. 22. The combined analysis of the 18 cases for

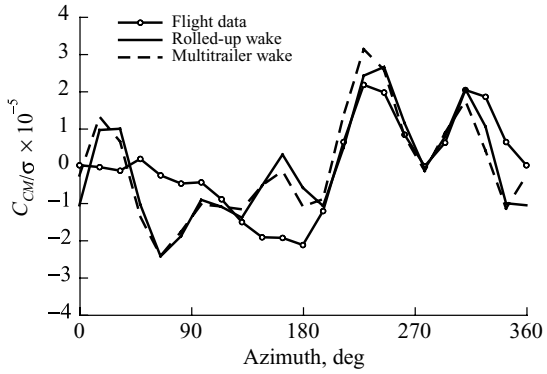

Fig. 20. Nondimensional chord bending moment as a function of azimuth on the SA 349/2 compared with CAMRAD II (Ref. 5); $r/R = 0.54$, $\mu = 0.361$.

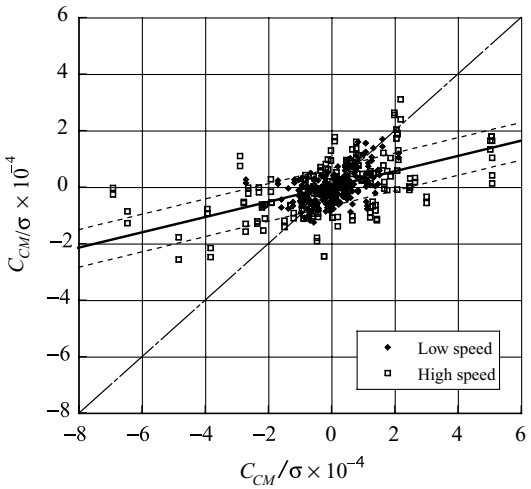

Fig. 21. Accuracy of CAMRAD II for combined analysis of midspan chord bending moment for five rotors at two airspeeds (Ref. 5); $m = 0.271$, $S_e = \pm 11\%$.

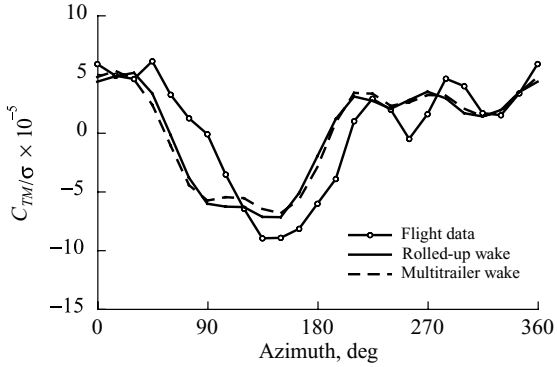

Fig. 22. Nondimensional torsion moment as a function of azimuth for the UH-60A compared with CAMRAD II (Ref. 5); $r/R = 0.30$, $\mu = 0.368$.

torsion moment is shown in Fig. 23. There is an underprediction of about 33% for these cases, which is comparable to the underprediction that was seen for the outboard pitching moments (see Fig. 17). If the combined analysis is done for the two airspeed regimes separately, there is little difference in the slopes: $m = 0.678$ at low speed and $m = 0.663$ at high speed. But as before, there is considerable variation between individual

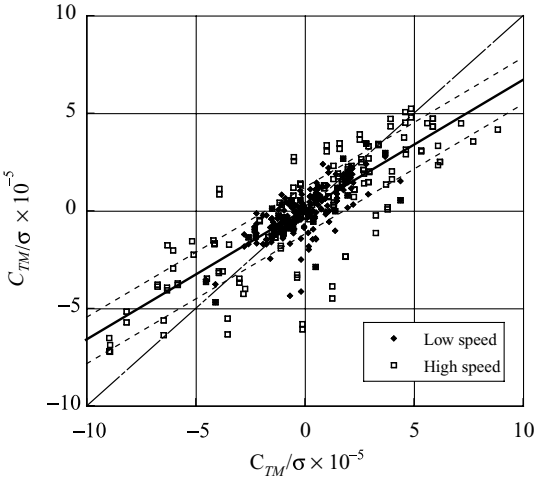

Fig. 23. Accuracy of CAMRAD II for combined analysis of midspan torsion moment for five rotors at two airspeeds (Ref. 5); $m = 0.665$, $S_e = \pm 12\%$.

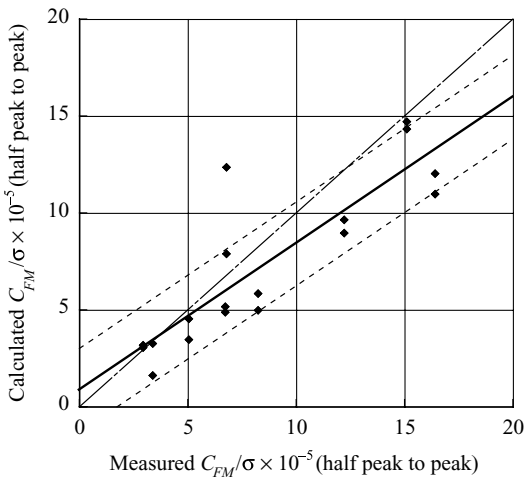

Fig. 24. Accuracy of CAMRAD II for half peak-to-peak flap bending moments for five rotors and two airspeeds (Ref. 5); $m = 0.756$, $S_e = \pm 11\%$.

cases, ranging from $m = 0.526$ for the Puma at high speed to $m = 0.879$ for the BO 105 at low speed.

The approach to evaluating predictive accuracy for the blade moments employed here uses the blade azimuth angle (time history) to provide a range of values for assessment. For the design engineer who is interested in fatigue damage, small differences in time histories are not of concern. Rather, it is the peak-to-peak loading that occurs over a wide range of conditions that is most meaningful. Using the Yeo and Johnson (Ref. 5) calculations and data, it is possible to compute the peak-to-peak loads for these same cases and assess the predictive accuracy based only on these peak-to-peak loads, as shown for the flap bending moments in Fig. 24. A comparison of the slopes and the standard errors for the flap and chord bending, and torsion moments using the time histories (referred to here as the azimuth approach) is compared with that obtained using the peak-to-peak data in Table 4. The slopes for flap bending and torsion moment accuracy are much the same for both approaches, although the scatter as indicated by S_e is less for the peak-to-peak assessment. The accuracy of the chord bending moment peak-to-peak prediction is improved as compared to the azimuth approach, but it remains inaccurate.

Table 4. Comparison of slope and standard error of estimate for azimuth and peak-to-peak approaches

	Flap		Chord		Torsion	
	m	S_e (%)	m	S_e (%)	m	S_e (%)
Azimuth	0.733	14	0.271	11	0.665	12
Peak to peak	0.756	11	0.409	9	0.674	7

Fixed-system loads

The measurement of the vibratory loads in the fixed system is extraordinarily difficult (as is the calculation). Gabel et al. (Ref. 12) used multiple approaches to measure vibratory loads in both the rotating and fixed systems, and their study illustrates many of the experimental difficulties. Sikorsky Aircraft tested a five-bladed bearingless rotor, the SBMR, in the 40- by 80-ft wind tunnel in 1992. The 5/rev loads were measured in the fixed system, and three different comprehensive analyses were used to predict these fixed-system loads (Ref. 13). The fixed-system measurements were obtained with a dynamically calibrated balance, and dynamic corrections were applied to the measured pitch-link loads as well. There were five components of the balance loads (all the forces and moments except torque), and the published results have unfortunately been normalized by an arbitrary factor. Three Sikorsky Aircraft analyses were compared with the measurement: two analyses developed by the company, KTRAN and RDYNE; and UMARC/S, a proprietary version of the University of Maryland's comprehensive analysis code. Figure 25 provides an example of the measurements of the 5/rev vertical force for the SBMR as a function of airspeed and includes the predictions of the three codes, which show widely differing predictions. A combined analysis of all load components and calculations is shown in Fig. 26. Such a combined analysis as shown here has serious limitations. For example, it is difficult to equate the 5/rev drag force with the 5/rev rolling moment, so the five load components are apples and oranges and different kinds of fruit. Moreover, because the loads have been normalized, the grouping for combined analysis is even less satisfactory. A more appropriate comparison is to look at each individual case as is shown in Table 5. There are only a few situations where a component of the balance load is predicted within ±25%; in most cases, the errors are much larger. But the scatter as measured by the standard error of estimate is good in most cases. Even for the most accurate code, UMARC/S, the predictions are poor.

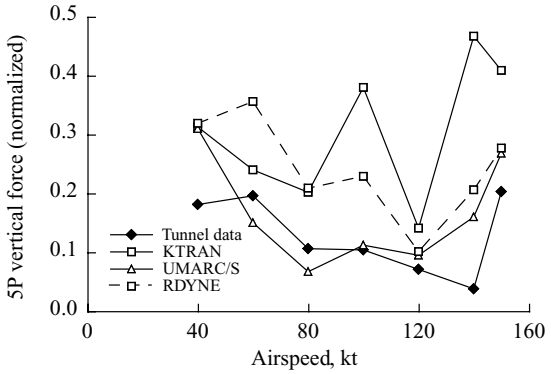

Fig. 25. Normalized 5/rev balance vertical force as a function of airspeed compared with three calculations (Ref. 13).

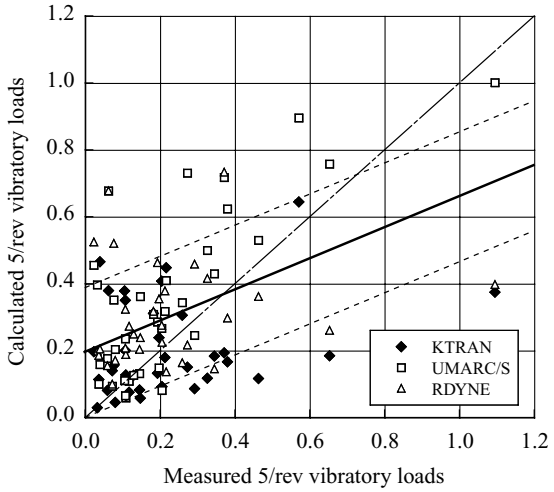

Fig. 26. Accuracy of Sikorsky analyses for the prediction of 5/rev balance loads (Ref. 13); $m = 0.465$, $S_e = \pm 16\%$.

Table 5. Comparison of slope and standard error of estimate for five components of balance loads using three Sikorsky Aircraft analyses

	KTRAN		UMARC/S		RDYNE	
Balance Load	m	S_e (%)	m	S_e (%)	m	S_e (%)
Drag force	0.331	2	0.678	20	0.614	7
Side force	0.197	3	1.557	8	0.306	8
Pitch moment	0.548	14	1.243	9	1.549	28
Roll moment	0.073	10	0.474	13	−0.210	10
Vertical force	−0.042	11	0.872	6	1.049	5

Wake and fuselage interactions

The rotor wake will cause loading on the fuselage, and the fuselage will change the inflow at the rotor. These interaction effects can be quite pronounced when they affect empennage loading or cause boundary layer separation. The CHARM code can represent a helicopter body using a panel method. Wachspress et al. (Ref. 14) have compared the CHARM code with the experimental data from a test of a model Dauphin rotor and fuselage. Figure 27 provides an example of the calculated and

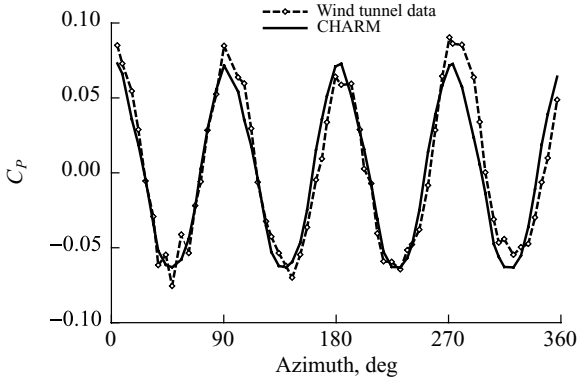

Fig. 27. Unsteady pressures on Dauphin fuselage from combined rotor and fuselage test, comparing CHARM calculations and measurements (Ref. 14).

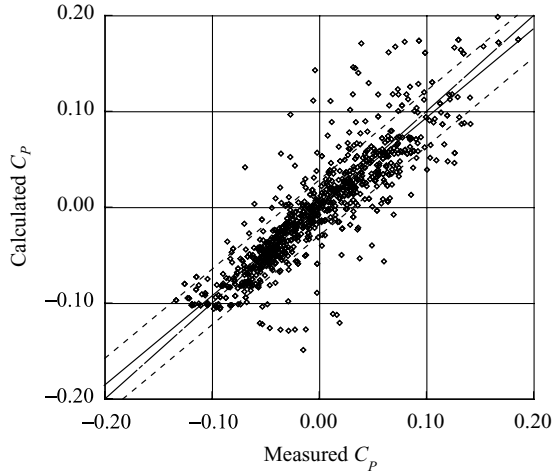

Fig. 28. Accuracy of CHARM predicted unsteady pressures for 15 locations on Dauphin fuselage (Ref. 14); $m = 0.929$, $S_e = \pm 15\%$.

measured unsteady pressure at a centerline location on the forward part of the fuselage. To assess the calculation, 15 pressure taps were used for the comparison: 5 were on the fuselage centerline, and 10 were on the fuselage sides at two longitudinal locations. Variation in the analysis variables was provided by sampling at various azimuths (as seen in Fig. 27) and using multiple pressure tap locations. Figure 28 shows the predictive accuracy of the CHARM analysis for the unsteady pressure prediction. The combined accuracy is quite good, with a 7% underprediction. The accuracy at individual stations ranged from $m = 0.677$ at a centerline location immediately behind the rotor hub to $m = 1.080$ at a centerline location on the empennage. Most of the individual slopes were close to $m = 0.9$.

Active controls

Tests of model- and full-scale rotors in recent decades have demonstrated a number of active control approaches that can reduce vibration and noise, including higher-harmonic control and individual blade control (IBC). In each of these demonstrations, some form of controller was used that measured vibratory loads and calculated the active control input that would provide a reduction. But few attempts have been made to correlate with these control inputs.

A full-scale BO 105 rotor with an IBC control system was tested in the 40- by 80-ft wind tunnel in two phases in 1993 and 1994 (Ref. 15). The active control in this test was a hydraulically actuated pitch link between the rotating swashplate and the blade root. Torok (Ref. 16) used a Sikorsky version of the UMARC code to predict the effects on 4/rev hub loads with changes in the pitch link 2/rev and 3/rev input phase angles. Because there was no calibrated dynamic balance, Torok computed the percent change in the loads rather than the actual loads themselves. Figure 29 shows the measured change in 4/rev hub shear with the variation in phase of the 2/rev input and compares this to the UMARC/S predictions. A combined analysis of the predicted changes in 4/rev hub shears, moments, and lift is shown in Fig. 30. Variation in the correlation variables is provided by the 2/rev and 3/rev input phase angles of the active pitch link, and the three components of hub loads. The predictive accuracy in this case, judged by the slope 0.939 for the combined analysis, is very good. But when the individual components are examined, as shown in Table 6, it is observed that most of the calculations are quite poor, only the 4/rev hub moment change to 3/rev phase inputs is within ±20% of the measurements. This example shows that caution

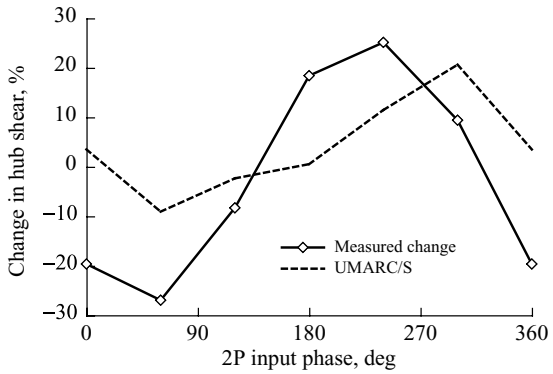

Fig. 29. Change in 4/rev hub shear as a function of IBC 2/rev input phase for BO 105 in the wind tunnel; comparison of measurements and UMARC (Ref. 16).

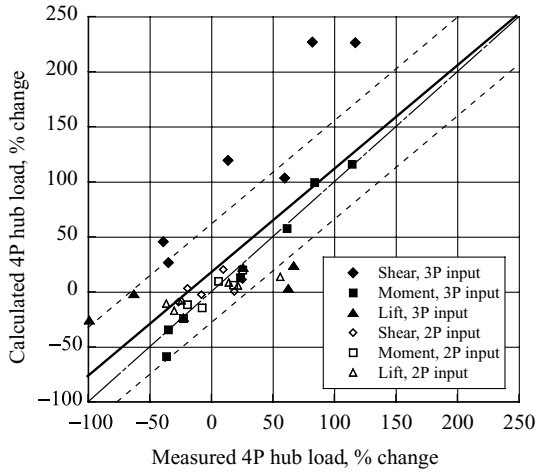

Fig. 30. Accuracy of UMARC/S prediction of 4/rev hub load change with variable 2/rev and 3/rev IBC inputs (Ref. 16); $m = 0.939$, $S_e = \pm 18\%$.

Table 6. UMARC/S predictive accuracy for changes in 4/rev hub loads with 2/rev and 3/rev input phase variation for full-scale BO 105 with IBC (Ref. 16)

Hub Component	Input	m
Shear	2/rev	0.310
Moment	2/rev	0.797
Lift	2/rev	0.318
Shear	3/rev	1.251
Moment	3/rev	1.126
Lift	3/rev	0.240

needs to be used in combining data sets for the quantitative approach presented here. Combining cases may be effective in some situations but misleading in others.

Aeromechanical/aeroelastic stability

There exists an extensive literature on aeroelastic and aeromechanical stability dating back to the earliest rotorcraft flight tests. For current rotorcraft designs, the major stability problems are those dealing with tiltrotor whirl stability and rotorcraft air and ground resonance.

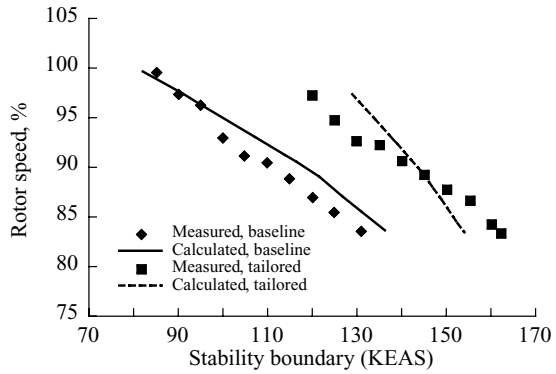

Fig. 31. Whirl flutter stability boundaries for two wing designs as tested in the Transonic Dynamics Tunnel compared with Bell Helicopter Textron's ASAP analysis (Ref. 17).

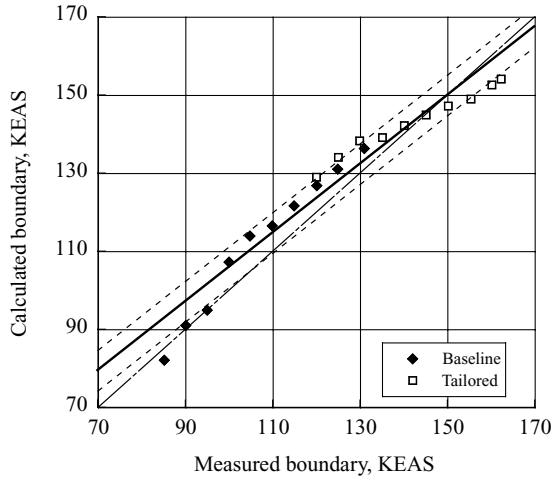

Fig. 32. Accuracy of ASAP prediction of whirl flutter stability boundaries for two wing designs (Ref. 17); $m = 0.880$, $S_e = \pm 3\%$.

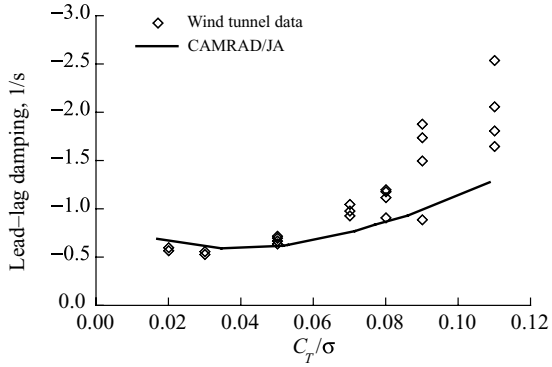

Fig. 33. Lead–lag damping of BO 105 in hover in 40- by 80-ft wind tunnel, compared with CAMRAD II (Ref. 18).

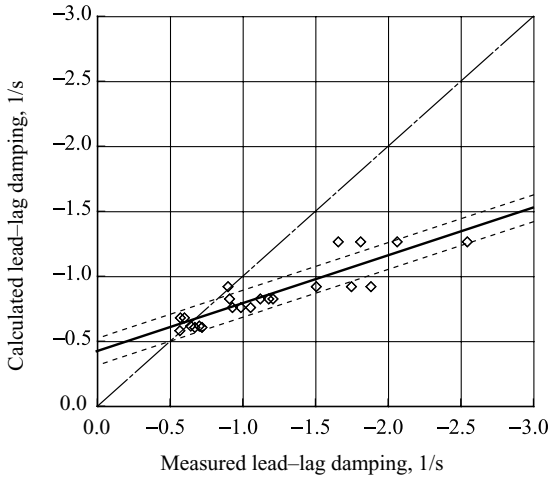

Fig. 34. Accuracy of CAMRAD II prediction of BO 105 lead–lag damping (Ref. 18); $m = 0.368$, $S_e = \pm 3\%$.

Bell Helicopter Textron has used their stability code, ASAP, to predict whirl stability boundaries for two wing designs tested at model scale in NASA Langley's Transonic Dynamics Tunnel (Ref. 17). Figure 31 shows the stability boundaries for the two wing designs. For each rotor speed, the boundary (in knots equivalent airspeed) where the damping becomes neutral is shown. The linear regression for these boundary points, where rotor speed is the source of the variation in the correlation variables, is shown in Fig. 32. The stability boundary is underpredicted by 12%. The scatter as indicated by the standard error of estimate is low.

Peterson and Johnson (Ref. 18) have compared the stability predictions of the comprehensive code CAMRAD/JA (a predecessor to CAMRAD II) with measurements obtained in hover (in the 40- by 80-ft wind tunnel) for a full-scale BO 105 rotor. Rotor thrust provided the variation in the correlation variables. The damping as a function of thrust is shown in Fig. 33. The linear regression analysis of these data is shown in Fig. 34. The damping is underpredicted, although the scatter in the results is low. To some extent, this is a typical result for aeromechanical stability testing since the accuracy of damping measurements is degraded at higher damping values. But even if half of the points in Fig. 33 were removed, those with the largest damping, the prediction would still be poor.

Concluding Remarks

A technique to quantitatively assess the predictive capability of aeromechanics methods has been described in this paper. The method considers some appropriate measurement to be the primary independent variable and the calculated result as the dependent variable. The linear regression of these variables is computed, and the slope of the regression line is considered a measure of accuracy. Perfect agreement would provide a slope of 1; values greater than 1 represent overprediction, whereas values less than 1 are underprediction. The standard error of estimate of the linear regression is a measure of scatter or dispersion, and in some cases may provide a better assessment of accuracy than the regression line slope. In a few cases, the offset of the linear regression provides a better indicator of error. For the technique to be useful in comparing computation and measurement, however, there must be significant variation in the dependent variables. The method is based on simple statistical methods that are readily available in any spreadsheet program or with any statistical software package.

Because the method is based on linear regression of data representing measurement and calculation, it is simple to apply over a wide range of problems as has been shown here. The correlation variables may not be strictly stochastic in all cases, and the use of simple statistical tools, such as linear regression, in this sense is a convenience.

But the problem of statistical independence looms large in combining data sets, as has been done here in multiple examples. It is considered a strength of the approach that it is possible to combine multiple cases, for example, two or three independent flight tests for performance or four or five separate tests for blade airloads. But each of these separate tests may have its own problems with differing error sources, and by combining the analysis of these independent tests, these differing error sources may be obscured.

The major emphasis in this paper has been on the accuracy of computation based on the slope of the resulting regression line. The slope is an absolute measurement and is particularly useful. But when expressing the standard error of the estimate or the offset, it is necessary to select a reference condition. In this paper the reference has been the figure's ordinate scale, but this is arbitrary.

A useful feature of the present approach when applied over a broad range of problems is that it describes a hierarchy of predictive accuracy. At the upper end of the hierarchy, such as for hover or forward flight performance, accuracies of the order of ± 1 or $\pm 2\%$ appear essential and scatter of $S_e > 3\%$ or 4% seems excessive. Lower down on the hierarchy, errors of $\pm 10\%$ in the prediction of fuselage unsteady pressures may be acceptable, and the best that can be presently done with blade airloads is of the order of $\pm 20\%$ or $\pm 30\%$. Similarly, stability predictions within $\pm 10\%$ or $\pm 20\%$ may be acceptable. Blade structural loads are more difficult to predict, vibratory loads are worse, and the prediction of fixed-system vibration is so difficult that it seems pointless to even call out a particular number.

The hierarchy of these problems may be useful in the sense that it can identify where further research is most needed. Performance predictions for conventional rotors are sufficiently accurate that additional progress can only be obtained with more accurate measurements than are currently obtained. On the other end of the hierarchy, it appears clear that increases in both analysis and measurement accuracy are required.

It has been shown here that phase errors in time histories tend to have significant effects upon both the slope and the standard error. When the phase errors are significant, then the use of the statistical measures used here become unreliable. This is possibly a benefit rather than a detriment of the approach, since phase errors are a clear indicator that the physics of the problem have not been captured.

The simplicity of the method shown here may have some utility in applications where extensive calculations are being made against many data sets, as sometimes occurs for CFD calculations. Rather than using extensive data visualization to compare calculation and data, the use of the present method may provide a guide as to where major problems in correlation are occurring and the analyst can then focus on these areas.

In addition, as experience is gained in applying this quantitative approach to additional data sets, it may be possible to develop benchmarks concerning the state of the art. If multiple cases in one topic area achieve a similar result, then it will be possible to establish a benchmark for the accuracy of the methods used. This benchmark can then guide further work, whether it be on the analytical or on the measurement side.

References

[1]Harris, F. D., Kocurek, J. D., McLarty, T. T., and Trept, T. J., Jr., "Helicopter Performance Methodology at Bell Helicopter Textron," American Helicopter Society 35th Annual Forum Proceedings, Washington, DC, May 21–23, 1979.

[2]Kocurek, J. D., Berkowitz, L. F., and Harris, F. D., "Hover Performance Methodology at Bell Helicopter Textron," American Helicopter Society 36th Annual Forum Proceedings, Washington, DC, May 13–14, 1980.

[3]Bousman, W. G., and Maier, T. H., "An Investigation of Helicopter Rotor Blade Flap Vibratory Loads," American Helicopter Society 48th Annual Forum Proceedings, Washington, DC, June 3–5, 1992.

[4]Bennett, R. L., "Panel 1: Prediction of Rotor and Control System Loads," *Rotorcraft Dynamics*, NASA SP-352, 1974.

[5]Yeo, H., Bousman, W. G., and Johnson, W., "Performance Analysis of a Utility Helicopter with Standard and Advanced Rotors," *Journal of the American Helicopter Society*, Vol. 49, (3), July 2004, pp. 250–270.

[6]Yeo, H., and Johnson, W., "Comparison of Rotor Structural Loads Calculated Using Comprehensive Analysis," 31st European Rotorcraft Forum, Florence, Italy, September 13–15, 2005.

[7]Felker, F. F., Quackenbush, T. R., Bliss, D. B., and Light, J. S. "Comparison of Predicted and Measured Rotor Performance in Hover Using a New Free Wake Analysis," American Helicopter Society 44th Annual Forum Proceedings, Washington, DC, June 16–18, 1988.

[8]Harris, F. D., "AHIP: The OH-58D from Conception to Production," American Helicopter Society 42nd Annual Forum Proceedings, Washington. DC, June 2–5, 1986.

[9]Kufeld, R. M., Balough, D. L., Cross, J. L., Studebaker, K. F., Jennison, C. D., and Bousman, W. G., "Flight Testing of the UH-60A Airloads Aircraft," American Helicopter Society 50th Annual Forum Proceedings, Washington, DC, May 11–13, 1994.

[10]Bousman, W. G., "Power Measurement Errors on a Utility Aircraft," American Helicopter Society Aerodynamics, Acoustics, and Test and Evaluation Technical Specialists Meeting, San Francisco, CA, January 23–25, 2002.

[11]Yeo, H., and Johnson, W., "Assessment of Comprehensive Analysis Calculation of Airloads on Helicopter Rotors," *Journal of Aircraft*, 42, 2005, pp. 1218–1228.

[12]Gabel, R., Sheffler, M., Tarzanin, F., and Hodder, D., "Wind Tunnel Modeling of Rotor Vibratory Loads," *Journal of the American Helicopter Society*, Vol. 28, (2), April 1983, pp. 47–54.

[13]Wang, J. M., and van Aken, J. M., "Correlation of Vibratory Hub Loads for a Sikorsky Full-Scale Bearingless Main Rotor," American Helicopter Society 50th Annual Forum Proceedings, Washington, DC, May 11–13, 1994.

[14]Wachspress, D. A., Quackenbush, T. R., and Boschitsch, A. H., "Rotorcraft Interactional Aerodynamics Calculations with Fast Vortex/Fast Panel Methods," American Helicopter Society 56th Annual Forum Proceedings, Virginia Beach, VA, May 2–4, 2000.

[15]Jacklin, S. A., Swanson, S., Blaas, A., Richter, P., Teves, D., Niesl, G., Kube, R., Gmelin, B., and Key, D. L., "Investigation of a Helicopter Individual Blade Control (IBC) System in Two Full-Scale Wind Tunnel Tests: Volume 1," NASA TP-2003-212276, 2003.

[16]Torok, M. S., "Aeroelastic Analysis of Active Rotor Control Concepts for Vibration Reduction," American Helicopter Society 52nd Annual Forum Proceedings, Washington, DC, June 4–6, 1996.

[17]Corso, L. M., Popelka, D. A., and Nixon, M. W., "Design, Analysis, and Test of a Composite Tailored Tiltrotor Wing," American Helicopter Society 53rd Annual Forum Proceedings, Virginia Beach, VA, April 29–May 1, 1997.

[18]Peterson, R. L., and Johnson, W., "Aeroelastic Loads and Stability Investigation of a Full-Scale Hingeless Rotor," International Forum on Aeroelasticity and Structural Dynamics, Aachen, Germany, 1991.